

CRITICAL IMPACT ANGLE FOR MITIGATING DEPOSITION OF SKIM MILK POWDER ON TUBES IN CROSS-FLOW

T.G. Walmsley, M.R.W. Walmsley, M.J. Atkins, J.R. Neale and D.M. Addenbrooke

Energy Research Centre, School of Engineering, University of Waikato, Hamilton, New Zealand
E-mail (Corresponding author): tgw7@waikato.ac.nz

ABSTRACT

Particulate fouling on the gas side of heat recovery equipment is a common industrial problem and its occurrence drastically degrades the thermal and hydraulic recuperator performance. The aim of this study is to characterize the deposition of Skim Milk Powder (SMP) on a single bare tube in cross-flow. Tubes tested include: round, elliptical, and turned square tube. A custom built rig is applied to simulate exhaust air conditions that is experienced in an exhaust exchanger. Results show that deposition mostly occurs on the front faces of the tubes with the rate of deposition decreasing through the duration of the test until equilibrium is reached. For a constant air flow rate, increasing particle stickiness resulted in greater deposition coverage around the front of the round and elliptical tubes whereas the turned square tube tended to be either clear or covered. On the round and elliptical tubes, the frontal deposit formed an apex shape. At equilibrium, the amount of deposition coverage on the tube varied depending on the tube shape, particle stickiness, and air velocity. Where deposition coverage stopped, the normal angle to the surface was calculated and has been shown to be well correlated to stickiness and less dependent of tube shape.

INTRODUCTION

Heat exchanger fouling is costly and affects a wide range of industries (Bott, 1995). Numerous studies have looked at the thermal and hydraulic impacts of fouling in many industrial settings, such as boilers, power stations, Heating, Ventilation and Cooling systems, to name only a few. In many situations, fouling can significantly degrade the thermal and hydraulic performance of heat exchangers. As fouling initiates and grows, it provides additional resistance to fluid flow increasing the system pressure drop and placing added electrical load on fans or pumps to maintain a constant flow rate. A fouling layer is also a barrier to heat transfer degrading the overall heat transfer film coefficient and exchanger duty.

A simple technique to reduce fouling has been to increase the fluid velocity resulting in higher fluid shear stresses at exchanger walls. For example, Stehlík (2011) reports that inserts have been placed between tubes in a tube bank as an attempt to increase fluid velocity and move the separation point of the fluid from the tube closer to the rear of the tube. Abd-Elhady et al. (2004) developed the concept of a dimensionless rolling moment, which is defined as the

hydrodynamic rolling moment divided by the adhesion resting moment, to calculate a limiting fouling velocity that theoretically predicts the onset of fouling. Estimates of the limiting fouling velocity for copper particles have been shown to be in close agreement with lab-scale experimental results (Jegla et al., 2010). However increasing velocity as a way to reduce fouling can dramatically increase the fluid pressure drop significantly increasing electrical load on fans and pumps.

Various heat exchanger geometries have been used to reduce fouling without adversely affecting the ratio of heat duty to pressure drop. For example, Zhang et al. (1992) investigated the application of a front row of “spoiler” tubes as a way to reduce deposition without significantly affecting heat exchanger pressure drop. A spoiler tube row is a non-heat transferring row of tubes placed in front of a tube bank, specifically designed to increase air turbulence and cause localized jetting. Recently, Abd-Elhady et al. (2011) demonstrated the effectiveness of using cone-shaped (a round tube with an apex on the front) tubes for reducing fouling yet increasing the heat transfer to pressure drop ratio. Paz et al. (2012) focused on fouling in diesel exhaust gases and showed the close relationship between wall shear stress and deposition. Using this link between wall shear stress and fouling, Walmsley et al. (2012b) developed Computational Fluid Dynamics (CFD) models to examine a wide range of tubes for their fouling, heat transfer and pressure drop characteristics.

Deposition of particles may result from a combination of several discrete transport processes and mechanisms (Guha, 2008). These processes are largely dependent on the dimensionless particle relaxation time (t^+), which is a function of the particle's density and radius and the fluid's density, viscosity, and wall shear stress. The particle relaxation time represents the time scale with which the particles respond to changes in the slip velocity. Typically, three general transport regimes are identified: (1) turbulent diffusion ($t^+ < 0.1$), (2) turbulent diffusion-eddy impaction ($0.1 < t^+ < 10$) and (3) particle inertia moderated ($t^+ > 10$). In the turbulent diffusion regime, deposition is a mass transport problem described by Fick's law. The second regime is a transitional regime whereas particles that fall in the particle inertia regime respond slowly to changes in velocity flow field changes as indicated by the large t^+ . Unpublished work by the authors has indicated that for milk powder deposition in heat exchangers, the dominant

transport regime is inertia moderated. The transport regime is important because it determines, to an extent, where deposition will occur.

The aim of this study is to experimentally characterize the deposition of Skim Milk Powder (SMP) on a single bare tube in cross-flow. Tube geometries include round, elliptical and turned square tubes. Using the findings of Paz et al. (2012), it is anticipated that localized wall shear stresses, in addition to particle surface stickiness, is related to deposition of milk powder particles. However, other studies, such as Murti et al. (2010) also suggest that the angle of entry through the shear layer and the impact angle of the particles on the tube surface may also be important.

The motivation for this work is to mitigate as far as possible the fouling of milk powder spray dryer exhaust recuperators through proper selection and design of the recuperator. Currently, exhaust heat recovery is seldom used for a number of reasons, the foremost one being the perceived process risk of unmanageable and excessive particulate fouling of the recuperator (Atkins et al., 2011). The overall goal is to provide empirical evidence that quantifies the effect of fouling on the thermal and hydraulic performance of these recuperators and minimizes these effects through good heat exchanger selection and design.

THEORY

Limiting Fouling Velocity

Based on the mean flow velocity a general parameter for predicting deposition is called the critical flow velocity. Abd-Elhady et al. (2011) define this as the mean flow velocity which results in a shear flow velocity sufficient to roll a deposited particle along a flat plate. This condition is met when the rolling moment ratio (RM) is equal to unity. The rolling moment ratio shown in Eq. 1 below is a balance of the hydrodynamic rolling moment caused by fluid drag and the adhesion resting moment, where the balance is about the point of contact between the particle and the surface.

$$RM = \frac{F_d (1.399 r_p - \alpha)}{(F_a + F_g - F_b - F_L) r_p} \quad (1)$$

This global parameter provides a mean flow velocity which ideally leads to no deposition. The practical use of this is to select a design velocity above this in order to prevent fouling. However the variables required to calculate RM are not easily determined and the global nature of the approach does not fully describe the nature of the particle deposition. While Eq. 1 applies to the rolling of a particle on a flat plate, this study is focused on mitigating deposition for different tube geometries. In the general case of a tube (excluding the turned square) the contribution of each force component in the moment balance is dependent on the location of deposition.

Critical Wall Shear Stress

Following on from the limiting flow velocity concept, a more localised parameter is the critical wall shear stress. Fig. 1 shows the modelled wall shear stress for round,

elliptical and turned square tubes. Paz et al. (2012) attempts to show how the localised wall shear stress provides a better description and tool for predicting when “rolling” occurs. They define the critical wall shear stress as the minimum shear stress value to cause RM to equal unity. Because the local wall shear stress of a tube in cross-flow varies around the profile of the tube, it is expected that any area with a wall shear stress above the critical value will experience no deposition.

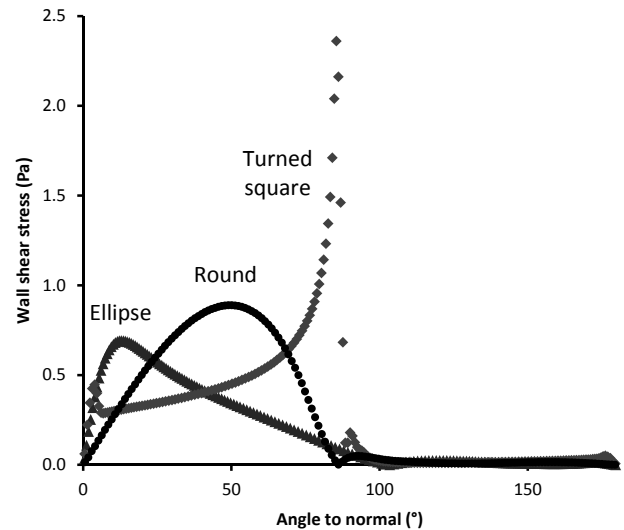


Fig. 1: Wall shear stress for round (a), elliptical (b) and turned squared (c) tubes using CFD. Data extracted from CFD models of single bare tubes in a duct. Refer to Walmsley et al. (2012b) for CFD parameters.

Critical Impact Angle

A parameter known as the “critical impact angle” of incidence (refer to Fig. 4) can be defined for describing the sticking/rebound behaviour of particles in oblique impact (Konstandopoulos, 2006). This is the angle beyond which no particles will stick to a surface. This concept is based on an energy balance between a particle’s tangential kinetic energy of impact and the minimum energy required to break its adhesive contact with the surface. Since the adhesion energy is related to particle stickiness, it is anticipated that the critical impact angle changes depending on the air conditions, which determine the particle stickiness.

UNDERSTANDING MILK POWDER STICKINESS

Many studies have shown that the stickiness behaviour of amorphous powders can be described by the extent to which the air temperature, T , exceeds the glass transition temperature, T_g , of the major amorphous components of the material (Palzer, 2005). For SMP the main amorphous component is lactose, which is about 52 wt% of SMP.

The glass transition temperature of lactose is usually determined using thermal methods such as Differential Scanning Calorimetry (DSC). Performing DSC on every sample of milk powder at each condition tested would be time consuming and highly impractical. However Brooks (2000) developed a third order empirical polynomial model for predicting the T_g of lactose at a given water activity (a_w), which is assumed to be in equilibrium with the air relative

humidity. This model is shown in Eq. 2 and is accurate for a_w in the range of 0 – 0.575.

$$T_g = -530.66(a_w)^3 + 652.06(a_w)^2 - 366.33(a_w) + 99.458 \quad (2)$$

For situations where the relative humidity is above 57.5% the Gordon and Taylor equation (Eq. 3) can be used to predict T_g . This equation uses the mass fractions of total solids and water (m_s and m_w respectively), the glass transition temperatures of lactose (T_{gl}) and water (T_{gw}), whose values were taken as 103 °C and -37 °C, and a constant, k , whose value was taken as 6.83.

$$T_g = \frac{T_{gl} + kX_w T_{gw}}{1 + kX_w}, \quad \text{where } X_w = \frac{m_w}{m_s} \quad (3)$$

Once the glass transition temperature has been calculated the parameter $T - T_g$ is then calculated. This value is correlated to the stickiness of the powder where a higher $T - T_g$ results in a higher stickiness (adhesiveness).

METHODOLOGY

The experimental setup for this study is shown in Fig. 2. The test rig allows milk powder to be added to an air stream of controlled temperature and humidity. This powder laden air flow is then contacted in cross-flow with various tube geometries. The air temperature is controlled using three separate thermal operations. First a plate-fin liquid to air heat exchanger circulates heated water to preheat air. The air is drawn in by a fan and blown along the test duct. A small amount of direct steam injection further increases the temperature of the air while achieving the target humidity. Finally an electric heater connected to a Variable Speed Drive (VSD) is used as a trimming element to adjust the final temperature of the air stream.

An orifice plate in the duct provides a pressure drop which is related to the air velocity in the air duct and used to control the fan speed to ensure a constant flow rate through the system as fouling on the tubes occurred. This also creates a region of low pressure immediately behind the plate where milk powder is injected, aided by a little suction induced by the orifice plate. The powder laden airflow then travels through the test duct where fully developed turbulent

flow is to be achieved before contact with the deposition surfaces. To control the rate of powder injection, a bottle full of powder is mechanically tapped. On average, powder was added at 3.8 g/min and test durations ranged from 20 to 80 minutes depending on the rate of deposition.

Round (25.4 mm), elliptical (22 mm x 39 mm), and turned square (25.4 mm x 25.4 mm) tubes were housed horizontally in a cross-flow fashion in a section with transparent acrylic walls enabling visual inspection of the test. Each tube was tested individually using various temperatures (46.3 °C to 62.4 °C) and humidities (46.6 % to 76.3 %) to achieve a range of powder stickiness levels. Photographs looking down the tubes were taken at regular intervals in an attempt to observe the growth of deposition over time. These images, depending on the clarity of the deposition layer, were later analysed to measure the location of deposition on each tube.

By adjusting the direct steam injection valve, it was attempted in the tests to achieve an absolute humidity of 50 g_{H2O}/kg_{Air} as this relates directly to the moisture content in industrial milk spray dryer exhausts. The process of setting up the initial temperature and humidity of the test system took anywhere up to three hours. Rigorous start-up and operation procedures for the equipment were established to prevent condensation on the tubes. In the event that condensation was evident on the tube, the results were invalidated. Preventing condensation is a key reason why it often took several hours to achieve the desired conditions because temperature and humidity increased had to be done by small increments. Once the desired values were achieved and steadied, powder was added. The time for separate tests varied depending on the rate of deposition.

Throughout the course of the tests, deposition, pressure drop across the tube, and air temperature and humidity are visually observed and/or monitored. In general a test would be stopped when the pressure drop across the tube reached a constant level. Temperature and relative humidity were logged at one second intervals and $T - T_g$ was calculated for each interval and averaged for the entire test period. At the conclusion of each test the tube assembly was removed from the test duct. Photographs were taken to show the deposition from various angles. Vernier callipers were then used to measure the projected width of the fouling on the tube.

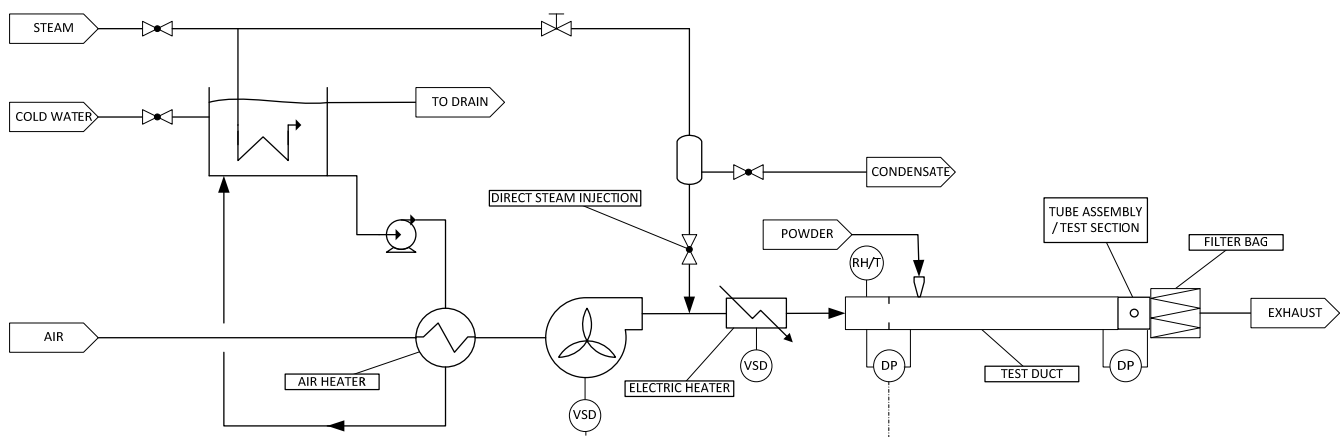


Fig. 2: Diagram of the experimental setup showing the numerous control elements.

Based on the photos, measurements and the tube geometry, the average location for the edge of the fouling layer was calculated using MatLab. This result was then compared with flow simulation CFD results (Fig. 1) to determine the wall shear stress at that location where deposition ceased. CFD model included a single tube in an 80 mm square duct (same as the experimental) using the modelling parameters outlined by Walmsley et al. (2012b). In addition the incident flow angle at that point was also calculated for comparison.

Subsequent test conditions were obtained by simply changing the setting on the heater VSD. As a result there is a change in temperature and relative humidity, which in effect produces a range of $T - T_g$ values. Once the system stabilised at a specific temperature and humidity, another test could be carried out.

Two average air velocities have been used in the deposition tests: 4.5 and 6.5 m/s. These velocities were selected to ensure the milk powder became entrained in the air with minimal settling and deposition at the bottom of the duct. Previous work by the authors (Walmsley et al., 2013, 2012a) has indicated that a relatively high exchanger face velocity is needed to help prevent fouling, reduce the heat exchanger area (due to an improved heat transfer air-side film coefficient), while gaining a substantial quantity of heat recovery.

A non-agglomerated Skim Milk Powder has been used in all tests. The particle size distribution was measured in iso-propanol using a Malvern Mastersizer 2000 according to the method of Pisecky (1997). By cumulative volume fraction, the mid diameter of the powder, $d(50\%)$, was measured as $104 \mu\text{m}$; $d(10\%) = 39 \mu\text{m}$ and $d(90\%) = 202 \mu\text{m}$.

RESULTS AND DISCUSSION

Critical Wall Shear Stress for Mitigating Deposition

The initial focus of this study was to investigate how the local wall shear stress around the profile of various tubes influenced particulate deposition. Three observations were expected in relation to this concept. First, it was expected that increasing $T - T_g$, i.e. stickiness, would require a higher wall shear stress to prevent deposition. If wall shear stress is a determining factor for deposition, then it is expected that the correlation between wall shear stress and $T - T_g$ is independent of the tube geometry and average bulk flow velocity. It was also expected that increasing the flow velocity would cause the deposition coverage to decrease in size for any given stickiness and for deposition to favour the rear facing side of the tube as shown in Paz et al. (2012).

Based on these hypotheses a unique critical wall shear stress should exist for each $T - T_g$ value. To test this hypothesis, the local wall shear stress at the location on the tube where deposition ceased is plotted against $T - T_g$ for round and elliptical tubes in Fig. 3. Results show no clear correlation for the tests performed at various face velocities. This lack of correlation suggests that the size and momentum of the milk powder particles, which is related to the particle relaxation time, is sufficiently large to break through the shear layer around the tubes with little sideways

movement. In addition, deposition at the rear of the tube was observed to be minimal. These results imply that the transport regimes of the bulk of the particles are inertia moderated rather than diffusion controlled. Estimations of the particle relaxation time place milk powder deposition in heat exchangers in the transitional and inertia moderated transport regimes.

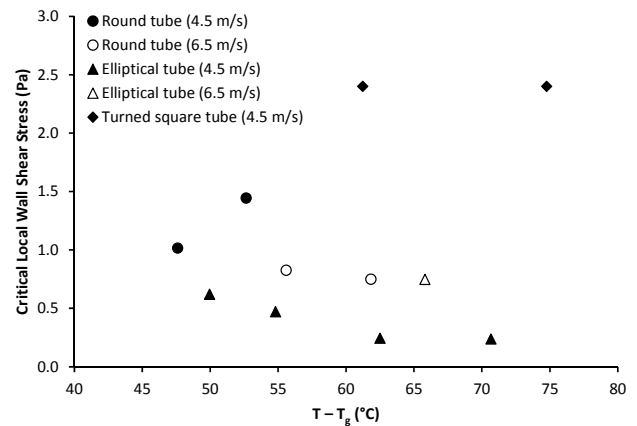


Fig. 3: Critical wall shear stress plotted against $T - T_g$ for the round and elliptical tubes showing no significant correlations.

Critical Impact Angle for Mitigating Deposition

In the situation where particle motion does not deviate from that of the bulk fluid, particles will impact the tube surface at an angle approximately equal to that of the bulk flow. Fig. 4 illustrates how the impact angle is calculated for the elliptical, round and turned square tubes.

The critical impact angle is defined as the angle between the bulk flow direction and the normal to the tube surface at the point where deposition terminates. For the round tube this is merely the angle of the polar coordinate at the surface location. For the elliptical tube the flow angle varies from that of the polar coordinate. However for the turned square tube the flow angle remains constant at 45° (considering only the positive angles).

Fig. 5 shows the critical impact angle plotted against the $T - T_g$ value for the round, elliptical and turned square tubes at 4.5 and 6.5 m/s. It can be seen that a critical impact angle of zero degrees occurs at $T - T_g \approx 44^\circ\text{C}$ and below this value very little deposition occurred. Above this lower $T - T_g$ limit the critical impact angle increased with a falling rate of growth as illustrated by the fitted first order exponential curve.

The regression model in Fig. 5 assumes that data for all the tubes at the different velocities follow the same trend indicating the impact angle on the tubes is a more dominant factor in determining whether powder deposits or not. For the round tube, an increase in bulk face velocity of 2 m/s (4.5 to 6.5 m/s) resulted in a 5°C increase in $T - T_g$.

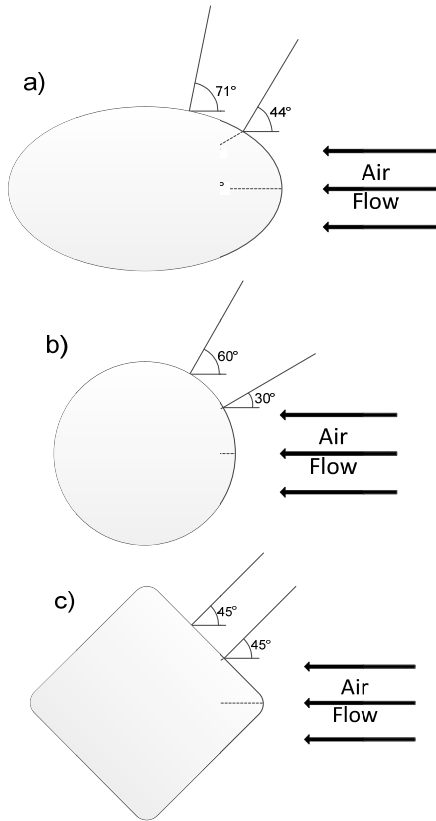


Fig. 4 Diagram showing how the critical impact angle is defined and how it changes for: a) elliptical tubes; b) round tubes; c) turned square tubes.

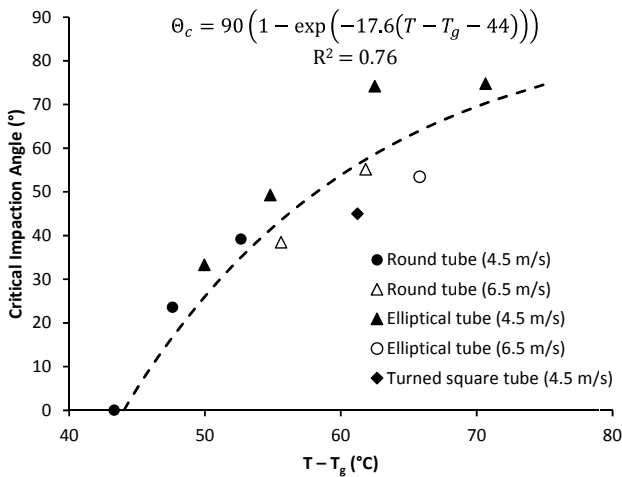


Fig. 5: Average critical impact angle for the turned square tube compared to the round and elliptical tubes.

Deposition Coverage for the Tube Geometries

Fig. 6 provides photographs of the end results of three tests performed on the round tube. Results are organised with the highest $T - T_g$ conditions at the bottom and lowest $T - T_g$ at the top. These results show that as the stickiness of the powder decreases the fouling layer and coverage over the front of the tube becomes smaller, causing the deposition to terminate at a smaller angle.

It was noticed in testing the turned square tube that no partial deposition occurred at intermediate $T - T_g$ values, as was seen for the round and elliptical tubes. Instead, there

was either no deposition, or a fouling layer completely covering the front face of the tube. This result is consistent with the idea that the impact angle is controlling deposition because the turned square has flat faces at an angle of 45° .

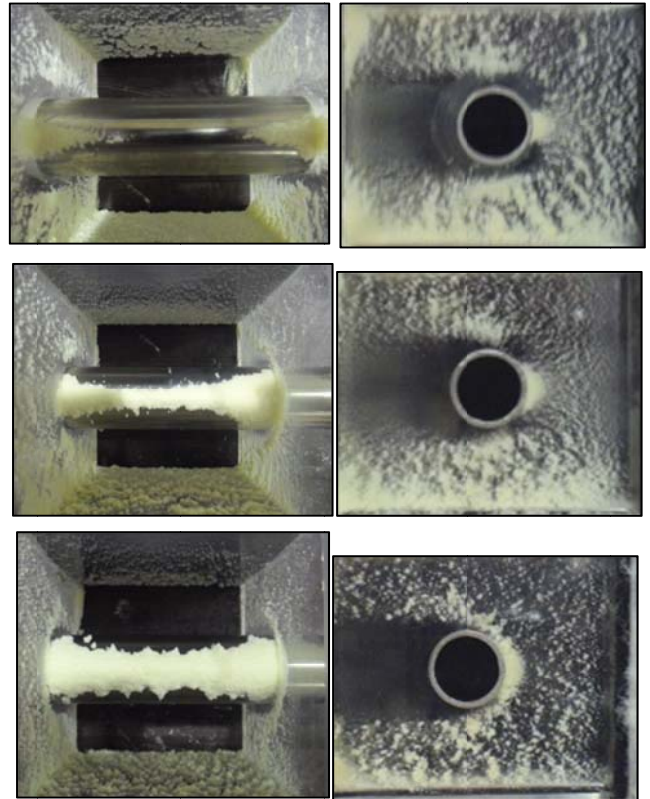


Fig. 6: The effect of increasing stickiness on the coverage of the fouling layer for round tube. From top, $T - T_g$ conditions are 43.3, 47.6 and 52.6 °C. Photographs were taken at the end of the test.

Observations confirmed that for the same stickiness conditions and bulk air velocity the coverage and amount of deposition on the elliptical tube is less than for the round tube. As a result the elliptical tube seems to be a favourable choice over the round tube in terms of fouling properties. Another benefit associated with the elliptical tube is the lower gas side flow resistance resulting in a lower pressure drop. A recent numerical evaluation of tube bundles confirms that for the same Reynolds number the pressure drop through an elliptical tube bundle is about 60 % lower than a bundle of round tubes and the heat transfer coefficient for elliptical tube is 20 – 30 % lower than round tube resulting in an overall increase in heat transfer to pressure drop ratio (Walmsley et al., 2012b).

The exponential regression model shown in Fig. 5 can be used to predict the average deposition coverage of the frontal tube area for a range of $T - T_g$ values as shown in Fig. 7 for all three tube geometries. It can be seen that for any given $T - T_g$ the round tube is expected to have a higher level of fouling than the ellipse as supported by observations.

In contrast to the round and elliptical tubes, the turned square tube only has the single impact angle of 45° . Particle deposition is predicted to only occur on the turned square

tube when the $T - T_g$ value is above $56\text{ }^\circ\text{C}$, which is lower than the experimental measure (Fig. 5). Therefore if the air conditions for any particular operation are below the critical stickiness then minimal deposition is expected to occur. However if air conditions move above the critical $T - T_g$ full deposition will occur on the turned square tube and continuous growth is likely up to a maximum amount when equilibrium is reached. A disadvantage of the turned square tube is its poor external flow behaviour. Of the three tubes tested, the turned square tube had the highest bare tube pressure drop by more than twice that of the round tube.

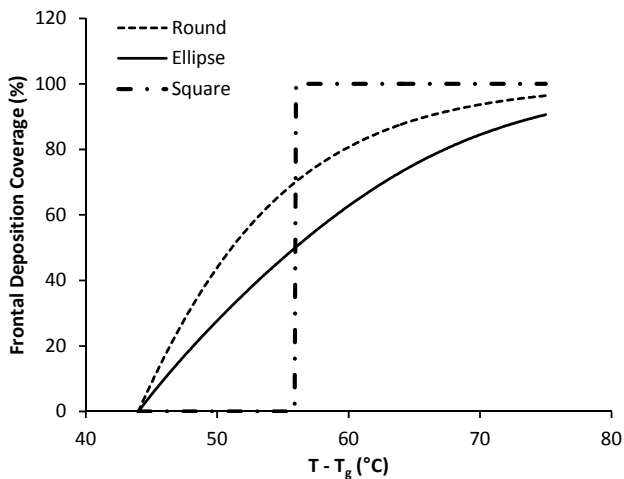


Fig. 7: Projected average deposition coverage area versus $T - T_g$ using the exponential regression of the round and elliptical tubes within the tested range.

Fouling Growth Rate and Pressure Drop

The fouling growth rate and pressure drop across the tube are related. Fig. 8 plots the pressure drop for the round tube over time for three stickiness levels that correspond to the photographs in Fig. 6. The data suggests the rate of pressure drop and, therefore, fouling build up is dependent on the stickiness level, with higher stickiness conditions resulting in faster growth. The rate of the pressure drop rise is also influenced by the rate of powder injection and any disturbance to the air flow rate, temperature and relative humidity. At $T - T_g$ of $47.6\text{ }^\circ\text{C}$, there was an issue with feeding the powder into the airflow, which resulted in an inconsistent injection rate causing a slightly different trend in the rate of pressure drop increase.

The pressure drop in Fig. 8 is asymptotic, although in many tests it was visually observed that the buildup of powder continued on the front of the tube, although at a reduced rate, after the pressure dropped leveled off. The deposition profile at the front of the tubes tended to be an apex.

Fig. 6 presents the photographs of the fouling layer build-up from the front and side view of the round tubes at the conclusion of three tests. From the side view, deposition can also be seen to protrude out from the front of the tube with no significant deposition on the rear of the tube. If a tube bundle is tested, it is possible that deposition on the back of tubes will occur due to the size of the recirculation at the rear of a tube inside a bundle is much smaller and tighter than for a single bare tube. Deposition on the wall of

the duct shows approximately where particles tend to stop impacting the tube. This wall deposition occurs due to cold wall temperatures increasing the localised stickiness conditions.

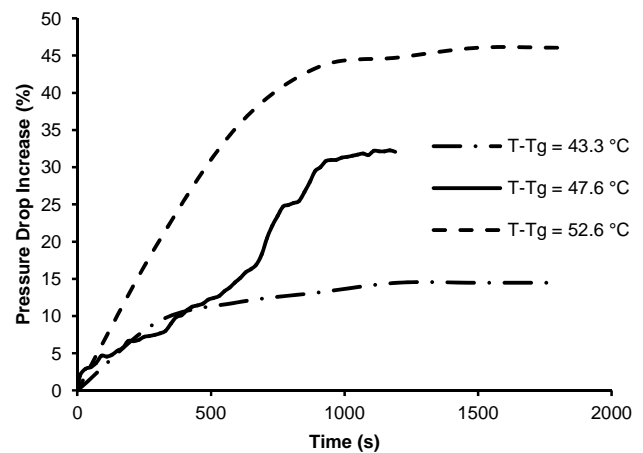


Fig. 8: Pressure drop over time across the round tube for three levels of stickiness.

CONCLUSIONS

The following points are the key conclusions from the work:

- Milk powder deposition occurs in the particle inertia moderated regime and is not strongly influenced by local wall shear stress for average duct velocities of 4.5 and 6.5 m/s.
- Deposition mostly occurs on the front face of the round, elliptical and turned square tubes and decreases around each tube until a critical impact angle to the surface of the tube and deposition ceases. None of the tube geometries contained significant deposition on the rear side of the tube.
- The critical impact angle is a function of particle stickiness (temperature and humidity) and air velocity, but independent of tube shape.
- Increasing particle stickiness with a duct air velocity of 4.5 m/s resulted in greater deposition coverage around the front of the round and elliptical tubes whereas the turned square tube tended to be either clear or covered.

ACKNOWLEDGEMENTS

The authors would like to thank the Todd Foundation in New Zealand for PhD scholarship funding and the support of the Energy Research Centre and the School of Engineering at the University of Waikato.

NOMENCLATURE

- a_w water activity, dimensionless
- DP differential pressure, Pa
- F force, N
- k material constant in Eq. 3, dimensionless
- m mass fraction, dimensionless
- r particle radius, μm
- RH relative humidity, %
- RM rolling moment, defined in Eq. 1, dimensionless
- t^+ particle relaxation time, dimensionless

T air temperature, °C
 T_g glass transition temperature, °C
 VSD variable speed drive
 X mass fraction of water on a dry basis, dimensionless
 α particle radius of deformation, m

Subscript

a adhesion
 b buoyancy
 cap capillary
 d drag
 ele electrostatic
 g gravity
 l lactose
 L lift
 p particle
 w water

REFERENCES

- Abd-Elhady, M.S., Rindt, C.C.M., Van Steenhoven, A.A., 2011. Influence of the apex angle of cone-shaped tubes on particulate fouling of heat exchangers. *Heat Transfer Engineering* Vol. 32, pp. 272 – 281.
- Abd-Elhady, M.S., Rindt, C.C.M., Wijers, J.G., Van Steenhoven, A.A., Bramer, E.A., Van der Meer, T.H., 2004. Minimum gas speed in heat exchangers to avoid particulate fouling. *International Journal of Heat and Mass Transfer* Vol. 47, pp. 3943–3955.
- Atkins, M.J., Walmsley, M.R.W., Neale, J.R., 2011. Integrating heat recovery from milk powder spray dryer exhausts in the dairy industry. *Applied Thermal Engineering* Vol. 31, pp. 2101–2106.
- Bott, T.R., 1995. Fouling of heat exchangers. Elsevier, Amsterdam, The Netherlands.
- Brooks, G.F., 2000. The sticking and crystallisation of amorphous lactose. M. Tech., Massey University, Palmerston North, New Zealand.
- Gordon, M., Taylor, J.S., 1952. Ideal copolymers and the second-order transitions of synthetic rubbers. i. non-crystalline copolymers. *J. Appl. Chem.* Vol. 2, pp. 493–500.
- Guha, A., 2008. Transport and deposition of particles in turbulent and laminar flow. *Annual Review of Fluid Mechanics* Vol. 40, pp. 311–341.
- Jegla, Z., Kilkovský, B., Stehlik, P., 2010. Calculation Tool for Particulate Fouling Prevention of Tubular Heat Transfer Equipment. *Heat Transfer Engineering* Vol. 31, pp. 757–765.
- Konstandopoulos, A.G., 2006. Particle sticking/rebound criteria at oblique impact. *Journal of Aerosol Science* Vol. 37, pp. 292–305.
- Murti, R.A., Paterson, A.H.J., Pearce, D., Bronlund, J.E., 2010. The influence of particle velocity on the stickiness of milk powder. *International Dairy Journal* Vol. 20, pp. 121–127.
- Palzer, S., 2005. The effect of glass transition on the desired and undesired agglomeration of amorphous food powders. *Chemical Engineering Science* Vol. 60, pp. 3959–3968.
- Paz, C., Suárez, E., Eirís, A., Porteiro, J., 2012. Experimental evaluation of the critical local wall shear stress around cylindrical probes fouled by diesel exhaust gases. *Experimental Thermal and Fluid Science* Vol. 38, pp. 85–93.
- Stehlik, P., 2011. Conventional versus specific types of heat exchangers in the case of polluted flue gas as the process fluid – A review. *Applied Thermal Engineering* Vol. 31, pp. 1–13.
- Walmsley, T.G., Walmsley, M.R.W., Atkins, M.J., Fodor, Z., Neale, J.R., 2012a. Optimal Stream Discharge Temperatures for a Dryer Operation Using a Thermo-Economic Assessment. *Chemical Engineering Transactions* 29, 403–408.
- Walmsley, T.G., Walmsley, M.R.W., Atkins, M.J., Hoffman-Vocke, J., Neale, J.R., 2012b. Numerical Performance Comparison of Different Tube Cross-Sections for Heat Recovery From Particle-Laden Exhaust Gas Streams. *Procedia Engineering* 42, 1476–1490.
- Walmsley, T.G., Walmsley, M.R.W., Atkins, M.J., Neale, J.R., 2013. Fouling and pressure drop analysis of milk powder deposition on the front of parallel fins. *Advanced Powder Technology* 24, 780–785.
- Zhang, G., Bott, T.R., Bemrose, C.R., 1992. Reducing particle deposition in air-cooled heat exchangers. *Heat Transfer Engineering* Vol. 13, pp. 81–87.